

# Stick boundary conditions and rotational velocity auto-correlation functions for colloidal particles in a coarse-grained representation of the solvent

J. T. Padding<sup>†</sup>, A. Wysocki<sup>‡</sup>, H. Löwen<sup>‡</sup> and A. A. Louis<sup>†</sup>

<sup>†</sup>Department of Chemistry, University of Cambridge, Lensfield Road, Cambridge CB2 1EW, United Kingdom

<sup>‡</sup>Institut für Theoretische Physik II, Heinrich-Heine-Universität Düsseldorf, Universitätsstraße 1, D-40225 Düsseldorf, Germany

**Abstract.** We show how to implement stick boundary conditions for a spherical colloid in a solvent that is coarse-grained by the method of stochastic rotation dynamics. This allows us to measure colloidal rotational velocity auto-correlation functions by direct computer simulation. We find quantitative agreement with Enskog theory for short times and with hydrodynamic mode-coupling theory for longer times. For aqueous colloidal suspensions, the Enskog contribution to the rotational friction is larger than the hydrodynamic one when the colloidal radius drops below 35nm.

PACS numbers: 82.70Dd

## 1. Introduction

Colloidal particles exhibit Brownian motion due to collisions with the molecules of the solvent in which they are suspended [1]. The resulting momentum transfer leads to translational diffusion of the colloidal positions. Because real colloids are not perfectly smooth or spherical, the solvent molecules can also transfer angular momentum, leading to rotational diffusion around the colloidal centres. Computer simulations of this process are difficult for two reasons: **1)** the length-scales of a typical colloid and a solvent differ by many orders of magnitude, for example, a colloid of radius  $1\mu\text{m}$  displaces  $1.4 \times 10^{11}$  water molecules, making direct simulations over meaningful length and timescales impossible in practice. **2)** Colloid-solvent interactions are usually taken to be radial, at least for a typical spherical colloidal particle, which means that angular momentum is not transferred from the solvent to the particle. In other words, the traditional implementation of molecular dynamics forces results in *slip boundary conditions* [2], whereas for a realistic colloid, local surface inhomogeneities would result in a tangential fluid velocity at the surface equal to the local velocity of the colloid surface, leading to *stick boundary conditions* [3].

The solution to problem **1)** is to coarse-grain the fluid to larger time and length-scales. There are many different ways of doing this, but in this paper we focus on stochastic rotation dynamics (SRD), a method first introduced by Malevanets and Kapral in 1999 [4]. SRD has the advantage that it includes thermal effects that dominate the short-time velocity auto-correlation functions, and also the

hydrodynamic forces that dominate at longer times. Briefly, SRD represents the solvent by ideal particles. To coarse-grain collisions, space is partitioned into cubic cells and in each one the particles exchange momentum with each other by rotating their velocity around the centre of mass velocity of the cell during a “collision” step. This procedure conserves momentum and kinetic energy, and thus generates the correct thermal Navier Stokes solutions in the thermodynamic limit. Its simplicity means that transport coefficients such as the viscosity can be calculated analytically [5, 6], facilitating the choice of simulation parameters.

Solute particles can also be coupled to the SRD solvent by treating solvent-solute and solute-solute interactions by a standard molecular dynamics scheme [7]. This method leads to slip boundary conditions for spherical colloids [8, 9], described as problem 2) above. To study rotational correlations, stick boundaries must be implemented, and how to do that is the subject of the present paper.

We proceed as follows: In the section 2, we briefly review our parameter choice for SRD. Section 3 describes how we implement stick boundary conditions for colloids while section 4 contains our simulation results for the linear and rotational velocity auto-correlation functions that verify our stick boundary implementation.

## 2. SRD model parameters

To simulate the SRD solvent, we follow our earlier implementation described ref [8]. Throughout this paper our results are described in units of SRD mass  $m$ , SRD cell size  $a_0$  and thermal energy  $k_B T$ . The number density (average number of SRD particles per SRD cell) is fixed at  $\gamma = 5$ , the rotation angle is  $\alpha = \pi/2$ , and the collision interval  $\delta t_c = 0.1 t_0$ , with time units  $t_0 = a_0(m/k_B T)^{1/2}$ ; this corresponds to a mean-free path of  $\lambda_{free} \approx 0.1 a_0$ . In our units these choices mean that the the fluid viscosity takes the value  $\eta = 2.5 m/a_0 t_0$  and the kinematic viscosity is  $\nu = 0.5 a_0^2/t_0$ . The Schmidt number  $Sc$ , which measures the rate of momentum (vorticity) diffusion relative to the rate of mass transfer is given by  $Sc = \nu/D_f \approx 5$ , where  $D_f$  is the fluid self-diffusion constant [5, 6]. In a gas  $Sc \approx 1$  – momentum is mainly transported by moving particles – whereas in a liquid it is much larger – momentum is primarily transported by interparticle collisions. For our purposes it is only important that vorticity diffuses faster than the particles do. With these parameters the Brownian time-scales are also well-separated [8]. If  $t_c$  is the time-scale over which the fluid loses memory of its velocity, and  $\tau_B$  is the time-scale over which the colloid loses memory of its initial velocity, and  $\tau_D$  is the time-scale over which the colloid diffuses over one radius  $a$ , then for the smallest colloids used, with radius  $a = 2$ ,  $\tau_B \approx 20 t_c$  and  $t_B < \tau_D \approx 200 t_c$ . For larger colloids the time-scales are separated even further. In contrast to earlier papers [7, 8, 9], the colloid-solvent interaction was not treated by a smooth potential which leads to slip boundary conditions. Instead, an effective hard-sphere radius was imposed, and the method of coupling the colloid to the solvent is described in the next section.

## 3. Stick boundary conditions for stochastic rotation dynamics

Stick boundary conditions imply that the tangential fluid velocity relative to an interface is zero at that interface [10]. The detailed molecular origins of these boundary conditions, or even the exact location at which they should be applied, are subtle problems [3]. For a recent review of the extensive literature on this subject see [11].

In some cases, such as a non-wetting surface, large effective slip lengths can occur [12], but for most colloidal applications the length-scales over which these more complex processes occur are coarse-grained out by methods such as SRD, so that simple stick boundary conditions should be sufficient.

Bounce-back collision rules, where the tangential component of the velocity relative to the surface of collision is reversed, could be used to implement stick boundary conditions. However, as Lamura *et al* [13] showed in their study of Poiseuille flow, the stochastic coarse-graining of the interparticle collisions together with the grid shift necessary for Galilean invariance[6] leads to a finite slip length at a planar wall, even when bounce-back rules are used. To fix this, they used the following prescription for cells that intersect the boundary: If number of SRD particles in a cell  $n_{\text{cell}}$  is smaller than the average number of SRD particles per cell in the bulk ( $\gamma$ ), they add the difference in virtual particles. In practice this means adding a Maxwellian velocity of variance  $(\gamma - n_{\text{cell}})k_B T/m$  for each Cartesian component, and setting the number density (for the calculation of the c.o.m. velocity) equal to  $\gamma$ . If the number of SRD particles is larger than  $\gamma$ , no virtual particles are added. We call this the Lamura rotation rule. It increases the effective friction for a planar wall, and indeed reduces the tangential velocity to nearly zero as required. That non-equilibrium effects can result in finite slip-lengths was shown as early as 1879 by James Clerk Maxwell [14], but his derivation results in a slip-length proportional to the Knudsen number, and these effects are an order of magnitude too small to explain the observed slip.

An alternative to the bounce-back rules is to use stochastic reflections where upon collision the particles are given a random normal velocity  $v_n$  and tangential velocity  $v_t$  taken from the following distributions:

$$P(v_n) \propto v_n \exp(-\beta v_n^2) \quad (1)$$

$$P(v_t) \propto \exp(-\beta v_t^2), \quad (2)$$

so that the wall acts as a thermostat [15]. Real colloids don't have perfectly smooth surfaces: there could be a grafted polymer brush for steric stabilisation, or an accumulation of co- and counter-ions for charge-stabilised suspensions. Fluid particles interacting with the surface would typically have multiple collisions with these local inhomogeneities, and stochastic boundary conditions can therefore be viewed as a coarse-grained representation of these processes. In that light, they appear more realistic than bounce-back rules, but whether that is important for either long-ranged hydrodynamic effects or for local Brownian motion is not clear. Inoue *et al* [16] first implemented such stochastic boundary conditions for SRD and more recently Hecht *et al* [17] used a similar, but more sophisticated, approach for spherical colloids.

We applied the Lamura rotation rule along the curved surface of a colloid (both reflection rules are equivalent), this is non-trivial because it is not obvious how to choose the distribution of the virtual particle velocities for a cell partially overlapping a colloid. All the implementations we tried resulted in rotational frictions that were too large. At present, the reasons for this are not completely clear, they may be related to the fact that the colloids can move, and therefore have a local temperature, in contrast to the walls used in [13], which are immobile.

For spherical colloids we finally used the following implementation of stochastic reflections, related to that used in [17]: If an SRD particle overlaps with a colloid, go half a time step back ( $-\mathbf{v} dt/2$ ), and place the particle along the shortest vector  $\mathbf{r}^*$  to the surface of the colloid. Then choose a random velocity  $\mathbf{v}'$  according to the stochastic distributions Eqs. (1) – (2), which are now centred around the local velocity of the

colloid surface, which is given by  $\mathbf{v}_{\text{loc}} = \mathbf{V} + \boldsymbol{\Omega} \times (\mathbf{r}^* - \mathbf{R})$ , where  $\boldsymbol{\Omega}$  and  $\mathbf{V}$  are the colloid rotation and velocity vectors. Complete the second half of the time step with that velocity ( $+\mathbf{v}' dt/2$ ). Add all momenta changes for the colloid:  $\Delta\mathbf{P} = \sum m(\mathbf{v}-\mathbf{v}')$ , as well as all its angular momenta changes:  $\Delta\mathbf{L} = \sum m(\mathbf{r}^* - \mathbf{R}) \times (\mathbf{v} - \mathbf{v}')$ . At the end of the time step, update the linear and angular velocity of the colloid according to  $\mathbf{V} \rightarrow \mathbf{V} + \Delta\mathbf{P}/M$  and  $\boldsymbol{\Omega} \rightarrow \boldsymbol{\Omega} + \Delta\mathbf{L}/I$ , where  $M$  is the mass and  $I = 2/5 Ma^2$  the moment of inertia a colloid for radius  $a$ . This method takes into account the fact that, on average, crossings take place at half a time-step. It proved to work slightly better than resetting the particle to the surface immediately, and then moving it with its new velocity for a full time step as done in ref. [17]. An exact calculation of impact time and place would be even better but this is computationally much slower. In any case, for small integration steps, there is not much difference between these different methods.

Finally, bounce back reflections can also be implemented, and give similar results to stochastic boundary conditions, but the latter were preferred because they locally thermostat the fluid, which may be important under flow conditions.

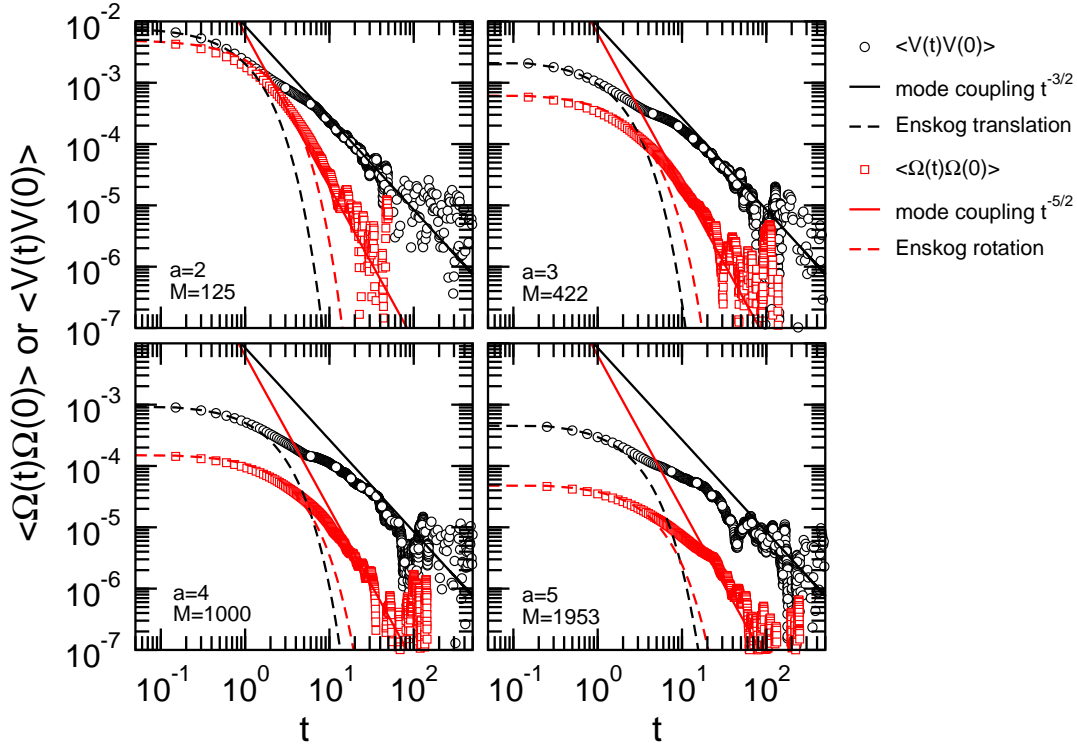


**Figure 1.** (colour online) Translational (circles) and rotational (squares) velocity autocorrelations for four different colloid radii. The x-axes are in units of  $t_0 = a_0(m/k_B T)^{1/2}$ , and the y-axes are in absolute units, e.g.  $\langle V(0)V(0) \rangle = k_B T/M = 1/125$  for  $a = 2$  etc. ... Solid lines are hydrodynamic mode-coupling predictions from Eqs. (9)–(10), dashed lines are short time Enskog friction predictions from Eqs. (3)–(6), and show good agreement with no free parameters. Note that for the smaller colloids, the Enskog and hydrodynamic regimes overlap substantially.

#### 4. Translational and rotational correlation functions

As a test of our stick-boundary conditions, we directly measure the translational velocity autocorrelation function (VACF), defined as  $\langle V(t)V(0) \rangle$ , where  $V(t)$  is a Cartesian component of the translational velocity of the colloidal particle at time  $t$ , as well as the rotational velocity autocorrelation (RVACF), defined as  $\langle \Omega(t)\Omega(0) \rangle$ , where  $\Omega(t)$  is a component of its rotational velocity. At  $t = 0$ , equipartition yields  $\langle V^2 \rangle = k_B T/M$  and  $\langle \Omega^2 \rangle = k_B T/I$ .

For short times, the correlation functions can be approximated using Enskog dense-gas kinetic theory, see e.g. [18, 19], which predicts the following exponential decay:

$$\lim_{t \rightarrow 0} \langle V(t)V(0) \rangle = \langle V^2 \rangle \exp(-\zeta_{\text{ENS}}^V t) \quad (3)$$

$$\lim_{t \rightarrow 0} \langle \Omega(t)\Omega(0) \rangle = \langle \Omega^2 \rangle \exp(-\zeta_{\text{ENS}}^\Omega t), \quad (4)$$

where the Enskog friction coefficients are given by

$$\zeta_{\text{ENS}}^V = \frac{8}{3} \left( \frac{2\pi k_B T m M}{m + M} \right)^{1/2} \frac{1}{M} \gamma a^2 \frac{1 + 2\chi}{1 + \chi} \quad (5)$$

$$\zeta_{\text{ENS}}^\Omega = \frac{8}{3} \left( \frac{2\pi k_B T m M}{m + M} \right)^{1/2} \frac{1}{M} \gamma a^2 \frac{1}{1 + \chi} \quad (6)$$

and  $\chi = I/(Ma^2) = 2/5$  is the gyration ratio. Note that  $\zeta_{\text{ENS}}^V/\zeta_{\text{ENS}}^\Omega = 1 + 2\chi = 9/5 > 1$ , so that the short time decorrelation of linear velocity is *faster* than the short time decorrelation of angular velocity, contrary to what would happen if one (erroneously) described the Brownian relaxation with hydrodynamic friction coefficients:

$$\zeta_h^V = 6\pi\eta a/M \quad (7)$$

$$\zeta_h^\Omega = 8\pi\eta a^3/I. \quad (8)$$

Using only these Stokes-Einstein frictions, one finds  $\zeta_h^V/\zeta_h^\Omega = 6\chi/8 = 3/10 < 1$ , which gives exactly the opposite effect (a difference of a factor 6)!

For the long time relaxation we can compare with hydrodynamic mode-coupling theory [20, 21] which predicts algebraic long-time tails of the form:

$$\lim_{t \rightarrow \infty} \langle V(t)V(0) \rangle = \frac{k_B T}{12m\gamma(\pi(\nu + D_c)t)^{3/2}} \quad (9)$$

$$\lim_{t \rightarrow \infty} \langle \Omega(t)\Omega(0) \rangle = \frac{k_B T \pi}{m\gamma(4\pi(\nu + D_c)t)^{5/2}} \quad (10)$$

where  $D_c$  is the colloidal diffusion constant which, in this case, is much smaller than the kinematic viscosity  $\nu$ , and can be ignored.

In Figure 3 we show VACF's and RVACF's for colloids of various radius  $a$ . We kept the colloid density constant (i.e.  $M \propto a^3$ ) and investigated four different sizes:  $a = 2$  ( $M = 125$ ),  $a = 3$  ( $M = 422$ ),  $a = 4$  ( $M = 1000$ ), and  $a = 5$  ( $M = 1953$ ). To keep finite-size corrections [22] small and comparable in each case, the box-size was varied to keep  $L/a = 24$  fixed. Thus the number of SRD particles varied from about  $5.5 \times 10^5$  for  $a = 2$  to  $8.6 \times 10^6$  for  $a = 5$ . We find excellent agreement with theory for the short-time behaviour, and good agreement for the long-time behaviour of the autocorrelation functions. For the smaller particles the statistics for the long-time tails are better than for the larger particles. Overall, these results suggest that our

coarse-grained method to implement stick boundary conditions leads to the correct physical behaviour.

Note that for the smallest colloid, the Enskog and hydrodynamic friction regimes are not clearly separated, especially for the rotational autocorrelation function. A naive parallel addition of the two types of friction to find the total friction  $\zeta$ :

$$\frac{1}{\zeta} = \frac{1}{\zeta_{ENS}} + \frac{1}{\zeta_h} \quad (11)$$

will therefore be incorrect, in particular for the rotational friction coefficient. For larger particles, this works better though, as shown in [9] where a similar analysis is performed for the translational friction coefficient of a colloidal particle with slip boundary conditions. Naively using only the Stokes-Einstein hydrodynamic frictions, i.e. assuming that the hydrodynamic radius is equal to the hard-sphere radius, will lead to important errors for small colloids. Consider the following example of a density matched colloid in an H<sub>2</sub>O solvent with viscosity  $\eta = 0.001$  Pa s at a temperature of 300K. Taking  $a$  in meters and  $\zeta$  in s<sup>-1</sup>, one finds  $\zeta_{ENS}^V = 764/a$  and  $\zeta_h^V = 4.5 \times 10^{-6}/a^2$  for translations and  $\zeta_{ENS}^\Omega = 5/9 \zeta_{ENS}^V = 424/a$  and  $\zeta_h^\Omega = 10/3 \zeta_h^V = 15 \times 10^{-6}/a^2$  for rotations. The physical radius at which the Enskog and hydrodynamic frictions are equal is given then by  $a_{crit}^V = 6$ nm for translations and  $a_{crit}^\Omega = 35.4$  nm for rotations. Because  $\zeta_{ENS}/\zeta_h \sim a$ , even for 100 nm the Enskog contribution to the rotational friction is of order 30% and cannot be ignored‡.

## Conclusions

We have shown how to implement stick boundary conditions for a colloid in a coarse-grained SRD solvent. Stochastic reflections with an approximate rule to determine the point where the SRD particle crossed the colloid surface was found to work best. This method was tested by explicit computer simulations of the translational and rotational velocity autocorrelation functions, which compare well to analytic calculations of the short-time behaviour via Enskog theory, and the long-time behaviour via mode-coupling theory. Our successful implementation of stick boundary conditions also shows that for small particles the Enskog and hydrodynamic effects are not clearly separated, and that the Enskog, or microscopic contribution[19], can be larger than the hydrodynamic one for small (nano) colloids, in particular for the rotational friction.

## Acknowledgements

JTP acknowledges support from the EPSRC and IMPACT FARADAY, and Schlumberger Cambridge Research. AAL acknowledges support from the Royal Society (London). AW and HL thank the the Deutsche Forschungsgemeinschaft (DFG), for support through the SFB-TR6 program ‘Physics of colloidal dispersions in external fields’.

## References

- [1] J. K. G. Dhont, *An Introduction to the Dynamics of Colloids*, Elsevier, (Amsterdam, 1996).

‡ The quantitative agreement with Enskog theory we find here may be due to the weaker correlations in the SRD fluid as compared to a full microscopic fluid. Because the SRD fluid and the boundary conditions are idealised, the exact radius where the microscopic Enskog friction and the hydrodynamic friction are equal will depend on further details of realistic physical systems.

- [2] J. R. Schmidt and J.L. Skinner, J. Chem. Phys. **119**, 8062 (2003).
- [3] L. Bocquet and J.-L. Barrat, Phys. Rev. E **49**, 3079 (1994).
- [4] A. Malevanets and R. Kapral, J. Chem. Phys. **110**, 8605 (1999).
- [5] N. Kikuchi, C. M. Pooley, J. F. Ryder, and J. M. Yeomans, J. Chem. Phys. **119**, 6388 (2003)
- [6] T. Ihle E. Tüzel and D. M. Kroll, Phys. Rev. E **70**, 035701(R) (2004).
- [7] A. Malevanets and R. Kapral, J. Chem. Phys. **112**, 7260 (2000).
- [8] J.T. Padding and A.A. Louis, Phys. Rev. Lett. **93**, 220601 (2004)
- [9] S.H. Lee and R. Kapral, J. Chem. Phys. **121**, 11163 (2004).
- [10] J. Happel and H. Brenner and *Low Reynolds Number Hydrodynamics : with special applications to particulate media* Springer ( New York 1983)
- [11] E. Lauga, M.P. Brenner, and H. Stone, in *Handbook of Experimental Fluid Dynamics*, Ed. J. Foss, C. Tropea and A. Yarin, Springer, New York (2005).
- [12] J.-L. Barrat, L. Bocquet, Phys. Rev. Lett. **82**, 4671 (1999).
- [13] A. Lamura, G. Gompper, T. Ihle and D.M. Kroll, Europhys. Lett. **56**, 319 (2001); *ibid* 768 (2001).
- [14] J. C. Maxwell Phil. Trans. Roy Soc, **170** (1879) 231-256. (see particularly the appendix)
- [15] J. L. Lebowitz and H. Spohn, J. Stat Phys. **19**, 633 (1978).
- [16] Y. Inoue, Y. Chen, and H. Ohashi, J. Stat. Phys. **107**, 85 (2002).
- [17] M. Hecht, J. Harting, T. Ihle and H. J. Herrmann, cond-mat/0502028
- [18] G. Subramanian and H.T. Davis, Phys. Rev. A, **11**, 1430 (1975).
- [19] J.T. Hynes, Annu. Rev. Phys. Chem. **f** 28, 301 (1977).
- [20] Ernst M. H., Hauge E. H. and van Leeuwen J. M. J., Phys. Rev. Lett., **25** 1254 (1970).
- [21] A.J. Masters and T. Keyes, J. Stat. Phys. **39**, 215 (1985).
- [22] V. Lobaskin and B. Dünweg, New J. Phys. **6**, 56 (2004).